Research Article

Received: 10 April 2015 Revised: 23 June 2015 Accepted article published: 10 July 2015 Published online in Wiley Online Library: 23 July 2015

(wileyonlinelibrary.com) DOI 10.1002/pi.4966

Synthesis and characterization of three-arm star-shaped conjugated poly(3-hexylthiophene)s: impact of the core structure on optical properties

Ha Tran Nguyen,[a,b*] Trung Thanh Nguyen,[a] Le-Thu T Nguyen,[a] Thang Van Le,[a,b] Viet Quoc Nguyen,[c] Thu Anh Nguyen[c] and Anh Tuan Luu[a]

Abstract

Star-shaped molecules consisting of regioregular poly(3-hexylthiophene) (P3HT) chains as the arms, attached to either a propeller-like triphenylamine or a planar triphenylbenzene core, have been synthesized via Suzuki coupling. The structures of the three-arm star-shaped poly(3-hexylthiophene) (s-P3HT) materials obtained were studied using Fourier transform infrared, ^{1}H and ^{13}C NMR, XRD, gel permeation chromatography and DSC. The s-P3HT polymers were soluble in common organic solvents and exhibited number-average molecular weights of 6000–7200 g mol^{-1}. Their optical properties in solutions and in solid state films were investigated using the UV–visible absorption and photoluminescence techniques, and were compared with those of linear P3HT.

Keywords: poly(3-hexylthiophene); triphenylamine; triphenylbenzene; star-shaped conjugated polymers; Grignard metathesis (GRIM) polymerization

INTRODUCTION

Extensive research has been devoted to the design and construction of nonlinear two- and three-dimensional conjugated macromolecules with star-shaped, disk-like and hyperbranched structures as multifunctional molecular architectures.[1–6] Normally, π-conjugated polymers and oligomers are one-dimensional chains with large anisotropy. This facilitates the efficient movement of charge carriers and excitons through the backbone when π-orbital delocalization occurs along the conjugated polymer chain.[6] However, the migration of these species in the two other directions is slowed down. Moreover, one-dimensional conjugated structures tend to be disordered in the bulk and show a large anisotropy in aligned systems. Hence, increasing the dimensionality of conjugated systems into a second dimension is often required.[7–11]

Star-shaped conjugated polymers are a class of nonlinear polymers. They have been paid much attention because of their compact structures and high segment densities. These features affect the crystalline, mechanical and electrical properties and give rise to interesting properties such as suppressed fluorescence quenching in the solid state and improved light-harvesting ability.[12–18] Generally, star-shaped conjugated polymers comprise several linear polymers as arms joined together through a central structure as a core. Depending on the bonds between the arms and the core, they can create one of several different shapes. If the arms are rigid-rod, a flat inflexible core normally provides an overall two-dimensional geometry, whereas a non-planar center results in a three-dimensional architecture. To prepare star-shaped conjugated polymers, there are two strategies: the arm-first method and the core-first method. In the arm-first method, linear arm polymers are synthesized first and subsequently end-group functionalized in order to be attached to a reactive core.[19–23] In contrast, the core-first method is used to prepare a reactive core that can initiate the polymerization of monomers to form arm chains.[24–26] Triphenylamine (TPA), triphenylbenzene (TPB) and their derivatives have been widely investigated as core units resulting in star-shaped conjugated polymers with good optical properties and p-type charge transport mobilities, which allow their use as hole-transport layers in organic field-effect transistors (OFET), organic solar cells (OSCs) as well as organic light emitting diodes.[27–30]

* *Correspondence to: Ha Tran Nguyen, Faculty of Materials Technology, Ho Chi Minh City University of Technology (HCMUT), Vietnam National University, 268 Ly Thuong Kiet, District 10, Ho Chi Minh City, Vietnam. E-mail: nguyentranha@hcmut.edu.vn*

a *Faculty of Materials Technology, Ho Chi Minh City University of Technology (HCMUT), Vietnam National University, 268 Ly Thuong Kiet, District 10, Ho Chi Minh City, Vietnam*

b *Materials Technology Key Laboratory (Mtlab), Vietnam National University – Ho Chi Minh City, 268 Ly Thuong Kiet, District 10, Ho Chi Minh City 70000, Vietnam*

c *National Key Laboratory of Polymer and Composite Materials – Ho Chi Minh City, University of Technology, 286 Ly Thuong Kiet Street, District 10, Ho Chi Minh City, Vietnam,*

In this respect, Paek *et al.*[31] have reported the synthesis via the arm-first method of star-shaped macromolecules with fused TPA as the core and three arms comprising dithieno(3, 2-b;20,30-d)silole, benzothiadiazole and hexylterthiophene units. These materials exhibited efficient p-type semiconducting performance in solution-processed OFETs with a hole mobility and on/off ratio of 7.6×10^{-3} cm^2 V^{-1} s^{-1} and 5×10^6, respectively. Niamnont *et al.*[29] have presented a series of TPA-based fluorophores containing multiple pyrene and corannulene, which were capable of detecting 2,4,6-trinitrotoluene on the nanogram per square centimeter scale. Recently, Hu *et al.*[32] have reported two novel star-shaped donor–acceptor small molecules with TPA as the core, benzothiadiazole as the arm, and alkyl cyanoacetate or 3-ethylrhodanine as the end-group. The films of these molecules exhibited broad absorption bands from 300 to 850 nm with optical bandgap around 1.6 eV. OSCs based on these materials had a power conversion efficiency of 1.79%.[32] On the other hand, regioregular poly(3-hexylthiophene)s (P3HTs) have attracted significant interest owing to their potential in a variety of applications including field-effect transistors, optical sensors, smart windows and OSCs.[33,34] A star-shaped P3HT has a different topology in comparison to a linear one, offering different characteristic physical properties such as chain aggregation, solubility, thermal and optical properties.[35] In addition, the star-shaped P3HT architectures are predicted to self-assemble into desirable nano-morphologies, thus giving a solution to the improper morphology issue of active layers in optoelectronic devices.[36] With this in mind, star-shaped P3HT materials are quite exceptional and provide an interesting subject for current research. However, a still unresolved problem associated with the synthesis of star-shaped P3HTs is mainly the lack of efficient synthetic strategies. Kiriy and coworkers[36] have presented the synthesis of a hairy P3HT by the core-first method. Nevertheless, the polydispersity of the obtained hairy polymer was quite broad, 1.98. More recently, Yuan *et al.*[35] have reported a synthetic route to prepare V- and Y-shaped P3HTs via difunctional and trifunctional Ni-complex-based initiators bearing biphenyl spacers, with narrow polydispersities of 1.1 as well as controlled molecular weights of 8.2 kDa. Despite significant efforts being made to enable the well-controlled synthesis of star-shaped P3HTs via the core-first approach, the finding of a suitable core-initiator and a preparation process for the Ni-complex-based core-initiator is challenging.

To address these issues, we synthesized via the arm-first method star-shaped P3HTs (s-P3HTs) comprising a TPA or a 1,3,5-triphenylbenzene (TPB) core and three branched motifs of P3HT. The s-P3HTs were prepared via Suzuki coupling reactions between a TPA/TPB derivative and α-bromo-poly(3-hexylthiophene) (Scheme 1). The synthesis and preliminary results on the characterization of the optical and thermal properties of the s-P3HTs are presented, together with a comparison with those of linear P3HT.

EXPERIMENTAL

Materials

3-Hexylthiophene was purchased from TCI (Tokyo, Japan). TPA and *N*-bromosuccinimide were purchased from Acros Organics (Bridgewater, NJ, USA). Tetrakis(triphenylphosphine) palladium(0) ($Pd(PPh_3)_4$) (99%), [1,1′-bis(diphenylphosphino) ferrocene]dichloropalladium(II) complex with dichloromethane ($Pd(dppf)Cl_2 \cdot CH_2Cl_2$) (99%), 4,4,4′,4′,5,5,5′,5′-octamethyl-2,2′-bi (1,3,2-dioxaborolane), 4-acetophenol and $K_2S_2O_7$ were purchased from Sigma-Aldrich (St. Louis, MO, USA). Potassium acetate (KOAc), sodium carbonate (99%) and magnesium sulfate (98%) were purchased from Acros (Bridgewater, NJ, USA) and used as received. Chloroform ($CHCl_3$) (99.5%), toluene (99.5%) and tetrahydrofuran (THF) (99%) were purchased from Fisher/Acros (Bridgewater, NJ, USA) and dried using molecular sieves under N_2. Dichloromethane (CH_2Cl_2) (99.8%), *n*-heptane (99%), methanol (99.8%), ethyl acetate (99%) and diethyl ether (99%) were purchased from Fisher/Acros (Bridgewater, NJ, USA) and used as received.

Measurements

^{1}H NMR and ^{13}C NMR spectra were recorded in deuterated chloroform ($CDCl_3$) with tetramethylsilane as an internal reference, on a Bruker Avance 300 MHz. Fourier transform infrared (FTIR) spectra, collected as the average of 64 scans with a resolution of 4 cm^{-1}, were recorded from a KBr disk on the FTIR Bruker Tensor 27.

SEC measurements were performed on a Polymer PL-GPC 50 gel permeation chromatography (GPC) system equipped with an RI detector, with THF as the eluent at a flow rate of 1.0 mL min^{-1}. Molecular weights and molecular weight distributions were calculated with reference to polystyrene standards.

Matrix-assisted laser desorption/ionization time-of-flight (MALDI-TOF) mass spectrometry was performed using a Waters QToF Premier mass spectrometer equipped with a nitrogen laser in reflection mode, using trans-2-[3-(4-tert-butylphenyl)-2-methylprop-2-enylidene]-malonitrile (DCTB) as a matrix. Nitrogen laser desorption at a wavelength equal to 337 nm was applied.

UV–visible absorption spectra of polymers in solution and polymer thin films were recorded on a Shimadzu UV-2450 spectrometer over the wavelength range 300–700 nm. Fluorescence spectra were measured on a Horiba IHR 325 spectrometer. DSC measurements were carried out with a DSC 204 F1 Netzsch instrument under nitrogen flow (heating rate 10 °C min^{-1}). TGA measurements were performed under nitrogen flow using a STA 409 PC Instrument with a heating rate of 10 °C min^{-1} from ambient temperature to 800 °C.

Wide-angle powder XRD patterns were recorded at room temperature on a Bruker AXS D8 Avance diffractometer using Cu Kα radiation ($k = 0.15406$ nm), at a scanning rate of 0.05° s^{-1}. The data were analyzed using DIFRAC plus Evaluation Package (EVA) software. The *d*-spacing was calculated from peak positions using Cu Kα radiation and Bragg's law.

Synthesis of 2-bromo-3-hexylthiophene (1)

To a solution of 3-hexylthiophene (5 g, 29.7 mmol) in anhydrous THF (50 mL) in a 200 mL flask, a solution of *N*-bromosuccinimide (5.29 g, 29.7 mmol) was added slowly at 0 °C under nitrogen. The mixture was stirred at 0 °C for 1 h. After that, 50 mL of distilled water was added to the reaction mixture, and the mixture was extracted with diethyl ether. The organic layer was washed with a solution of $Na_2S_2O_3$ (10%), and then the mixture was washed with a solution of KOH (10%) and dried over anhydrous $MgSO_4$. The mixture was distilled to give a colorless oil (6.7 g, 92% yield).

^{1}H NMR (300 MHz, $CDCl_3$), δ (ppm): 7.19 (d, 1H), 6.82 (d, 1H), 2.59 (t, 2H), 1.59 (quint, 2H), 1.33 (m, 6H), 0.91 (t, 3H). ^{13}C NMR (75.5 MHz, $CDCl_3$), δ (ppm): 141.0, 128.2, 125.1, 108.8, 31.6, 29.7, 29.4, 28.0, 22.6, 14.1.

Synthesis of 2-bromo-3-hexyl-5-iodothiophene (2)

Iodine (1.42 g, 11.18 mmol) and iodobenzenediacetate (1.965 g, 6.1 mmol) were added to a solution of 2-bromo-3-hexylthiophene

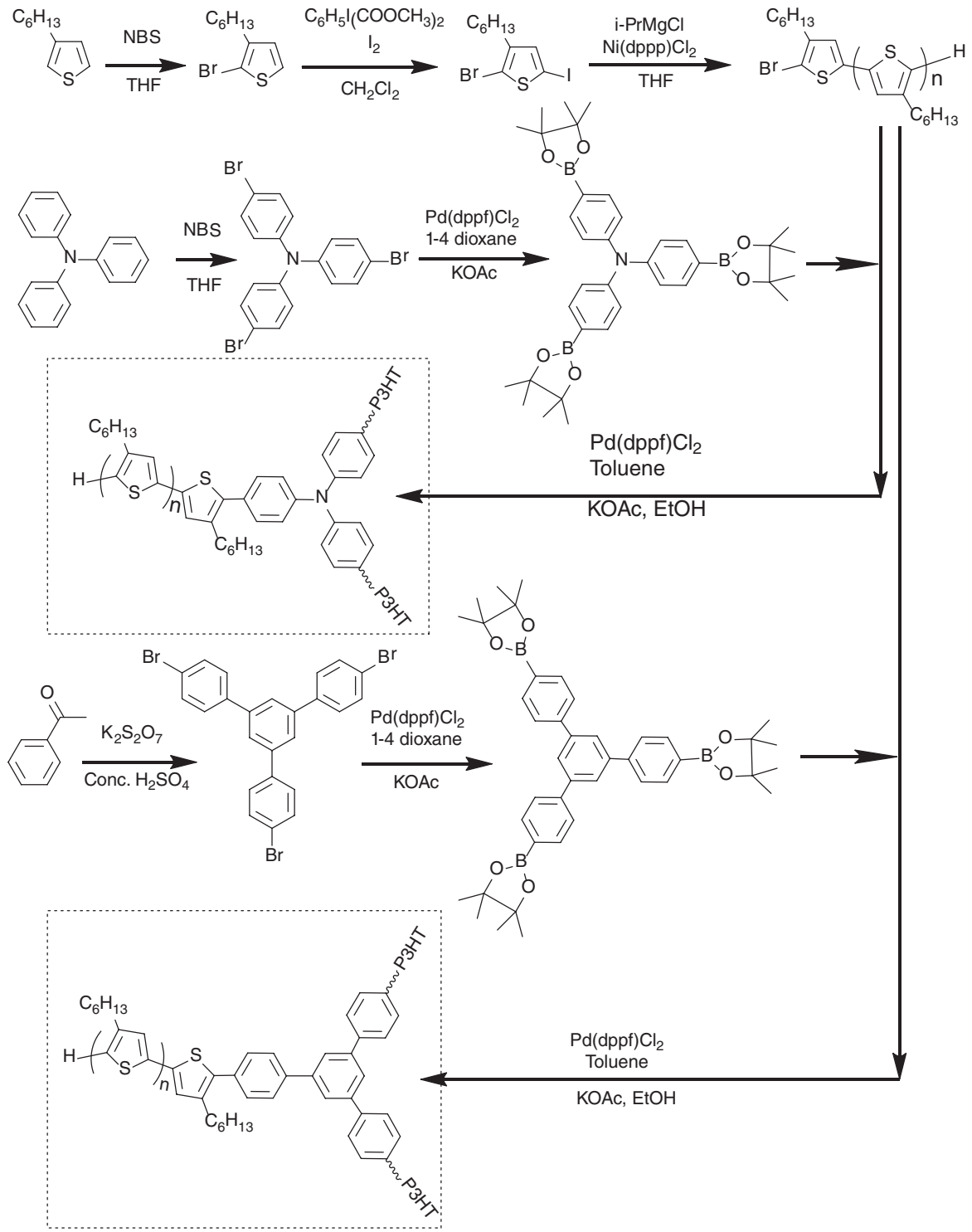

Scheme 1. Synthesis of s-P3HT-TPA and s-P3HT-TPB.

(**1**) (2.5 g, 11.1 mmol) in CH_2Cl_2 (25 mL) at 0 °C. The mixture was stirred at room temperature for 4 h. Then, aqueous $Na_2S_2O_3$ (10%) was added, and the mixture was extracted with diethyl ether and dried over anhydrous $MgSO_4$. The solvent was evaporated to obtain a crude product. The residue was purified by silica column chromatography (eluent *n*-heptane) to give pure 2-bromo-3-hexyl-5-iodothiophene (**2**) as a pale yellow oil (3 g, 86% yield).

^{1}H NMR (300 MHz, $CDCl_3$), δ (ppm): 6.97 (s, 1H), 2.52 (t, 2H), 1.56 (quint, 2H), 1.32 (m, 6H), 0.89 (t, 3H). ^{13}C NMR (75.5 MHz, $CDCl_3$), δ (ppm): 144.3, 137.0, 111.7, 71.0, 31.5, 29.6, 29.2, 28.8, 22.5, 14.1.

Synthesis of regioregular head-to-tail poly(3-hexylthiophene) with H/Br end-groups (3)

A dry 500 mL three-neck flask was flushed with nitrogen and charged with 2-bromo-3-hexyl-5-iodothiophene (**2**) (15 g,

40 mmol). After three azeotropic distillations by toluene, anhydrous THF (220 mL) was added via a syringe, and the mixture was stirred at 0 °C for 1 h. i-PrMgCl (2 mol L^{-1} solution in THF, 19.14 mL, 38.28 mmol) was added via a syringe and the mixture was continuously stirred at 0 °C for 1 h. The reaction mixture was kept cool at 0 °C. The mixture was transferred to a flask containing a suspension of Ni(dppp)Cl_2 (760 mg, 1.4 mmol) in THF (25 mL). The polymerization was carried out for 24 h at 0 °C, followed by addition of a 5 mol L^{-1} HCl solution. After termination, the reaction was stirred for 15 min and extracted with $CHCl_3$. The polymer was precipitated in cold methanol and washed several times with *n*-hexane. The polymer was characterized by ^{1}H NMR and GPC. The yield was 70%.

FTIR (cm^{-1}): 721, 819, 1376, 1454, 1510, 2853, 2922, 2953. ^{1}H NMR (300 MHz, $CDCl_3$), δ (ppm): 6.96 (s, 1H), 2.90 (t, 2H), 1.79 (sex, 2H), 1.52 (q, 6H), 0.94 (t, 3H). GPC: $M_n = 4500$ g mol^{-1}. $Đ = M_w/M_n = 1.18$. *m/z*: 1409, 1574, 1740, 1906, 2072, 2238, 2404, 2570, 2736, 2902.

Synthesis of tris(4-bromophenyl)amine (4)

N-bromosuccinimide (2.17 g, 12.2 mmol) and triphenylamine (1 g, 4.08 mmol) were added to anhydrous THF (10 mL) at 0 °C under nitrogen. The mixture was stirred at 50 °C for 1.5 h. After completion of the reaction, 10 mL of distilled water was added to the reaction mixture, which was extracted with CH_2Cl_2. The organic layer was washed with a 10% solution of $Na_2S_2O_3$ and a 10% solution of KOH, dried over anhydrous $MgSO_4$ and concentrated. The product was precipitated in cold *n*-heptane and dried under vacuum to give a white powder ($R_f = 0.6$; yield 67%).

^{1}H NMR (300 MHz, $CDCl_3$), δ (ppm): 7.35 (d, 6H), 6.95 (d, 6H). MS *m/z* (M+) 478. Analysis calculated for $C_{18}H_{12}Br_3N$: C, 45.1; H, 2.51; Br, 49.49; N, 2.92. Found: C, 45.35; H, 2.41; Br, 49.35; N, 2.89.

Synthesis of tris(4-(4,4,5,5-tetramethyl-1,3,2-dioxaborolan-2-yl)phenyl)amine (dioxaborolane-TPA) (5)

Tris(4-bromophenyl)amine (**4**) (1 g, 2.075 mmol) and 4,4,4′,4′,5,5,5′,5′-octamethyl-2,2′-bi(1,3,2-dioxaborolane) (1.58 g, 6.225 mmol) were dissolved in 30 mL of 1,4-dioxane. To this solution, 169 mg (10 mol%) of Pd(dppf)$Cl_2 \cdot CH_2Cl_2$ and 0.61 g (6.225 mmol) of KOAc were added, and the solution was bubbled with N_2 for 30 min. Then, the reaction was carried out at 85 °C for 24 h. After completion of the reaction, 100 mL of ethyl acetate was added for dilution and the mixture was filtered through Celite to remove the Pd catalyst. The solution obtained was washed with distilled water (2 × 100 mL) and with 10% aqueous solution of $Na_2S_2O_3$ (2 × 100 mL). Afterwards, the solution was dried over $MgSO_4$, and the solvent was evaporated to obtain a black liquid as the crude product. The crude product was purified over a silica column with *n*-heptane/ethyl acetate (v/v 5/5) as eluent to obtain a white powder as the pure product tris(4-(4,4,5,5-tetramethyl-1,3,2-dioxaborolan-2-yl)phenyl)amine (**5**) ($R_f = 0.6$; yield 56%).

^{1}H NMR (300 MHz, $CDCl_3$), δ (ppm): 7.7 (d, 2H), 7.10 (d, 2H), 1.35 (s, 12H). MS *m/z* (M^+) 623. Analysis calculated for $C_{36}H_{48}B_3NO_6$: C, 69.34; H, 7.70; B, 5.29; N, 2.24; O, 15.40. Found: C, 68.67; H, 7.81; B, 5.31; N, 2.17; O, 15.93.

Synthesis of 1,3,5-tris(4-bromophenyl)benzene (6)

4-Bromoacetophenone (5 g, 25.13 mmol), 0.25 mL of H_2SO_4 (conc.) and $K_2S_2O_7$ (6.6 g, 26.14 mmol) were heated at 180 °C for 16 h under a nitrogen atmosphere. The resulting crude solid was cooled to room temperature and refluxed in 25 mL of dry ethanol (EtOH) for 1 h and then cooled to room temperature. The solution was filtered and the resulting solid was refluxed in 25 mL of H_2O to give a pale yellow solid that was then filtered. The crude product was dried under vacuum giving 7.5 g of dried product, which was recrystallized from $CHCl_3$ (yield 55%).

^{1}H NMR (300 MHz, $CDCl_3$), δ (ppm): 7.53 (d, 6H), 7.60 (d, 6H), 7.68 (s, 3H). MS *m/z* (M^+) 539. Analysis calculated for $C_{24}H_{15}Br_3$: C, 53.34; H, 2.77; Br, 43.89. Found: C, 53.25; H, 2.69; Br, 44.06.

Synthesis of 1,3,5-tris(4-(4,4,5,5-tetramethyl-1,3,2-dioxaborolan-2-yl)phenyl)benzene (dioxaborolane-TPB) (7)

1,3,5-tris(4-bromophenyl)benzene (**6**) (1 g, 1.84 mmol) and 4,4,4′,4′,5,5,5′,5′-octamethyl-2,2′-bi(1,3,2-dioxaborolane) (1.4 g, 5.52 mmol) were dissolved in 30 mL of toluene. To this solution, 150 mg (10 mol%) of Pd(dppf)$Cl_2 \cdot CH_2Cl_2$ and 0.54 g (5.52 mmol) of KOAc were added, and the solution was bubbled with N_2 for 30 min. Then, the reaction was carried out at 85 °C for 24 h. After completion of the reaction, 100 mL of CH_2Cl_2 was added for dilution and the mixture was filtered through Celite to remove the Pd catalyst. The solution obtained was washed with distilled water (2 × 100 mL) and with 10% aqueous solution of $Na_2S_2O_3$ (2 × 100 mL). Afterwards, the solution was dried over $MgSO_4$, and the solvent was evaporated to obtain a black liquid as the crude product. The crude product was purified over a silica column with *n*-heptane/ethyl acetate (v/v 7/3) as eluent to obtain a solid as the pure product 1,3,5-tris(4-(4,4,5,5-tetramethyl-1,3,2-dioxaborolan-2-yl)phenyl) benzene (**7**) ($R_f = 0.6$; yield 51%).

^{1}H NMR (300 MHz, $CDCl_3$), δ (ppm): 7.93 (d, $J = 8.2$ Hz, 2H), 7.82 (s, 1H), 7.71 (d, $J = 8.2$ Hz, 2H), 1.37 (s, 12H). MS *m/z* (M^+) 684. Analysis calculated for $C_{42}H_{51}B_3O_6$: C, 73.68; H, 7.45; B, 4.82; O, 14.03. Found: C, 73.89; H, 7.31; B, 4.73, O, 13.96.

Synthesis of star-shaped conjugated polymer based on regioregular poly(3-hexylthiophene) and triphenylamine moieties (s-P3HT-TPA) (8)

100 mg (0.022 mmol) of poly(3-hexylthiophene) (**3**) was dissolved in 60 mL of toluene. Then, tris(4-(4,4,5,5-tetramethyl-1,3,2-dioxaborolan-2-yl)phenyl)amine (**5**) (4.62 mg, 7.4×10^{-3} mmol) in toluene (40 mL) was dropped slowly at 100 °C for 8 h. To the solution, 23.5 mg (0.17 mmol) of K_2CO_3 was added. Then, 0.084 mL of EtOH and 0.065 mL of distilled water were introduced to the solution. The mixture was bubbled with N_2 for 30 min, followed by addition of 2.8 mg of Pd(dppf)$Cl_2 \cdot CH_2Cl_2$. The reaction was carried out at 100 °C for 24 h. After completion of the reaction, the mixture was extracted with $CHCl_3$. The organic layer obtained was passed through Celite to remove the Pd catalyst and any trace of insoluble polymer fraction, and subsequently washed with a 10% solution of $Na_2S_2O_3$ and distilled water, dried over Na_2CO_3, concentrated and finally poured into a large amount of cold methanol/ethyl acetate (v/v 6/4) to precipitate the polymer. The resulting polymer was isolated by filtration and was re-dissolved in CH_2Cl_2. A small amount of an insoluble fraction was removed by filtration. The filtrate was collected, concentrated and precipitated in cold *n*-heptane to recover the polymer, which was then continuously washed with acetone to remove the unreacted tris(4-(4,4,5,5-tetramethyl-1,3,2-dioxaborolan-2-yl)phenyl)amine (**5**) and oligomers. The purified product was finally dried under reduced pressure at 50 °C for 24 h. A yield of 93% was obtained.

FTIR (cm^{-1}): 721, 819, 1376, 1454, 1510, 2853, 2922, 2953. ^{1}H NMR (300 MHz, $CDCl_3$), δ (ppm): 7.61 (s, 2H), 6.96 (s, 1H), 6.81 (s, 2H), 2.90

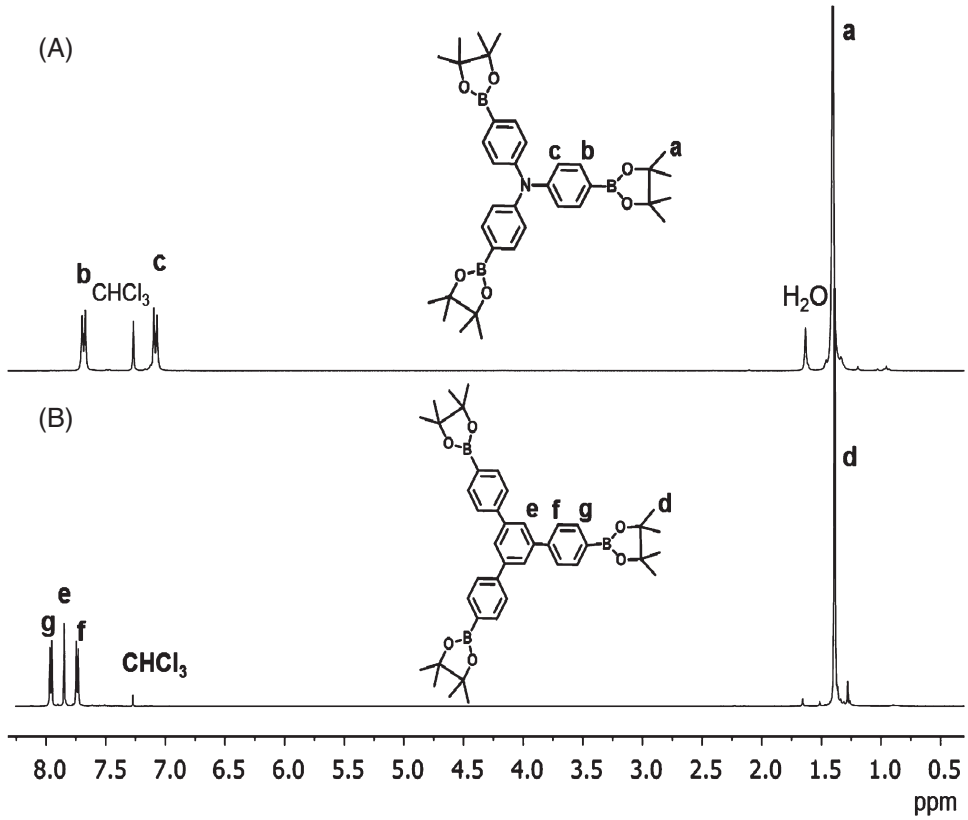

Figure 1. ^{1}H NMR spectra of tris(4-(4,4,5,5-tetramethyl-1,3,2-dioxaborolan-2-yl)phenyl)amine (**5**) (A) and 1,3,5-tris(4-(4,4,5,5-tetramethyl-1,3,2-dioxaborolan-2-yl)phenyl)benzene (**7**) (B).

(t, 2H), 1.79 (sex, 2H), 1.52 (q, 6H), 0.94 (t, 3H). ^{13} C NMR (75.5 MHz, $CDCl_3$), δ (ppm): 143.5, 141.0, 135.5, 129.5, 127.0, 126.0, 119.0, 32.0, 30.5, 29.0, 22.5, 14.0. GPC: $M_n = 6000$ g mol^{-1}. $Đ = M_w/M_n = 1.55$.

Synthesis of star-shaped conjugated polymer based on regioregular poly(3-hexylthiophene) and triphenylbenzene moieties (s-P3HT-TPB) (9)

100 mg (0.022 mmol) of poly(3-hexylthiophene) (**3**) was dissolved in 60 mL of toluene. Then, 1,3,5-tris(4-(4,4,5,5-tetramethyl-1,3,2-dioxaborolan-2-yl)phenyl)benzene (**7**) (5.01 mg, 7.4×10^{-3} mmol) in toluene (40 mL) was dropped slowly at 100 °C for 8 h. To the solution, 20 mg (0.143 mmol) of K_2CO_3 was added. Then, 0.07 mL of EtOH and 0.05 mL of distilled water were introduced to the solution. The mixture was bubbled with N_2 for 30 min, followed by addition of 3 mg of Pd(dppf)$Cl_2 \cdot CH_2Cl_2$. The reaction was carried out at 100 °C for 24 h. After completion of the reaction, the mixture was extracted with $CHCl_3$. The organic layer obtained was passed through Celite to remove the Pd catalyst and the insoluble polymer fraction, and subsequently washed with a 10% solution of $Na_2S_2O_3$ and distilled water, dried over Na_2CO_3, concentrated and finally poured into a large amount of cold methanol/ethyl acetate (v/v 6/4) to precipitate the polymer. The resulting polymer was isolated by filtration and was re-dissolved in CH_2Cl_2. A small amount of an insoluble fraction was removed by filtration. The filtrate was collected, concentrated and precipitated in cold *n*-heptane to recover the polymer, which was then continuously washed with acetone to remove the unreacted 1,3,5-tris(4-(4,4,5,5-tetramethyl-1,3,2-dioxaborolan-2-yl)phenyl) benzene and oligomers. A yield of 91% was obtained.

FTIR (cm^{-1}): 721, 819, 1376, 1454, 1510, 2853, 2922, 2953. ^{1}H NMR (300 MHz, $CDCl_3$), δ (ppm): 7.60 (s, 1H), 7.48 (m, 2H), 7.43 (m, 2H), 6.96 (s, 1H), 6.81 (s, 2H), 2.90 (t, 2H), 1.79 (sex, 2H), 1.52 (q, 6H), 0.94 (t, 3H). ^{13} C NMR (75.5 MHz, $CDCl_3$), δ (ppm): 141.0, 135.5, 131.6, 129.0, 127.0, 120.5, 32.0, 30.5, 29.0, 22.5, 14.0. GPC: $M_n = 7200$ g mol^{-1}. $Đ = M_w/M_n = 1.23$.

RESULTS AND DISCUSSION

Synthesis and characterization

The synthetic route for linear P3HT and the star-shaped P3HTs containing either triphenylamine or triphenylbenzene as the core is shown in Scheme 1. First, linear P3HT was synthesized via a controlled 'quasi-living' Grignard metathesis (GRIM) polymerization of 2-bromo-5-iodo-3-hexyl thiophene monomers in the presence of Ni(dppp)Cl_2 to form α-bromo-poly(3-hexylthiophene) (Br-P3HT-H). As far as the GRIM polymerization is concerned, treatment of 2-bromo-5-iodo-3-hexylthiophene with 1 equivalent of i-PrMgCl resulted in a magnesium – iodine exchange reaction, also referred to as the GRIM reaction. Then, the 'activated monomer' was polymerized in the presence of Ni(dppp)Cl_2 using an initial monomer-to-nickel molar ratio of 30. The polymerization was performed in THF at 0 °C for 24 h and quickly terminated by addition of a 5 mol L^{-1} HCl solution to prevent any transhalogenation side-reaction. A good correlation between the theoretical molecular weight ($M_{nth} = 4890$ g mol^{-1}) and the value determined by GPC ($M_{nexp} = 4500$ g mol^{-1}) was obtained, attesting to control over the GRIM polymerization. This was further confirmed by a symmetrical and narrow molecular weight distribution characterized by

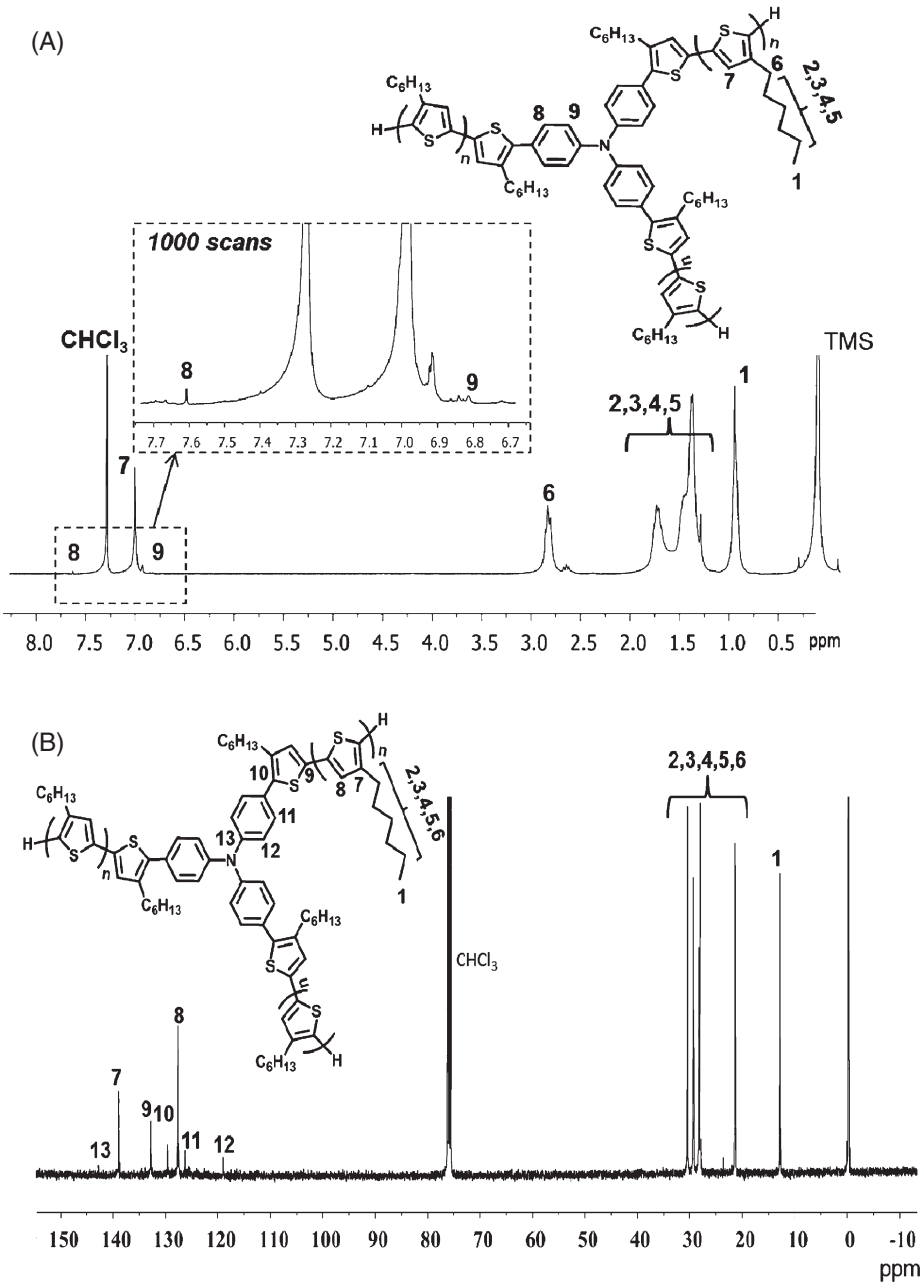

Figure 2. ^{1}H NMR (A) and ^{13}C NMR (B) spectra of s-P3HT-TPA.

a low polydispersity index ($Đ = 1.18$). A high regioregularity content of 99% was determined by ^{1}H NMR, while the presence of the expected end-groups (H/Br) was fully evidenced by MALDI-TOF analysis.

On the other hand, tris(4-(4,4,5,5-tetramethyl-1,3,2-dioxaborolan-2-yl)phenyl)amine (**5**) was synthesized with a yield of 40% from triphenylamine over two steps of bromination and borylation reactions. Similarly, 1,3,5-tris(4-(4,4,5,5-tetramethyl-1,3,2-dioxaborolan-2-yl)phenyl)benzene (**7**) was synthesized from 4-acetophenol with a yield of 30%. As shown in Fig. 1, the ^{1}H NMR spectra of the synthesized compounds reveal characteristic peaks corresponding to the structures of the TPA and TPB dioxaborolane derivatives.

Then, s-P3HT-TPA (**8**) was prepared with a yield of 93% via the standard Suzuki coupling reaction between P3HT (**3**) and dioxaborolane-containing TPA (**5**). To obtain a high reaction conversion, in our case a P3HT (4500 g mol^{-1}) to dioxaborolane-TPA molar ratio of 1 to 0.3 was established. The formation of s-P3HT-TPA was controlled by slow addition of a diluted solution of (**5**) at 100 °C in the presence of the Pd(dppf)$Cl_2 \cdot CH_2Cl_2$ complex as catalyst in anhydrous toluene. To define the star-like structure of the polymers in many cases is a complicated task. However, in this work, ^{1}H and ^{13}C NMR peak assignment and integration were obvious. As shown in the ^{1}H NMR spectrum of s-P3HT-TPA in Fig. 2(A), in the aromatic region, besides the signals of internal thienyl rings (6.96 ppm), the signals of the TPA core group at 7.61 ppm and 6.81 ppm are also observed. A comparison of the ^{1}H NMR spectra of s-P3HT-TPA and dioxaborolane-TPA (**5**) showed that the peak at 7.10 ppm (Fig. 1(A), peak c) attributed to the protons of the benzene ring adjacent to the amine core of TPA

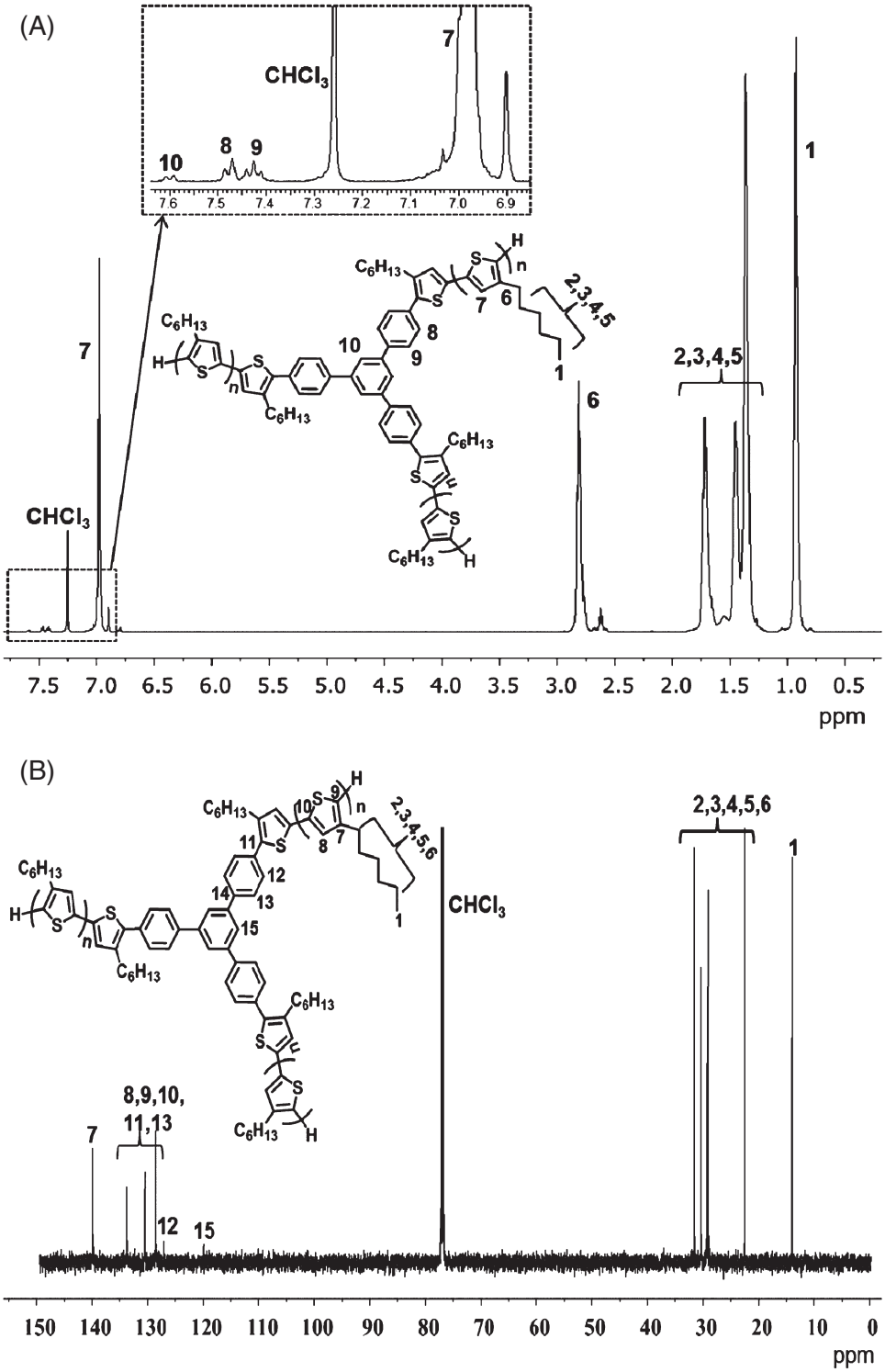

Figure 3. ^{1}H NMR (A) and ^{13}C NMR (B) spectra of s-P3HT-TPB.

was shifted to 6.81 ppm for s-P3HT-TPA (Fig. 2(A), peak 9). In agreement with this, the peak assigned to the protons of the benzene ring adjacent to the dioxaborolane group of dioxaborolane-TPA (**5**) at 7.70 ppm (Fig. 1(A), peak b) was shifted to 7.61 ppm (Fig. 2(A), peak 8) for s-P3HT-TPA. These results suggest that the Suzuki coupling reaction took place between dioxaborolane-TPA (**5**) and the Br end-group of P3HT to form s-P3HT-TPA. It should be noted that the crude reaction product may contain unreacted linear P3HT chains and two-arm species, besides the three-arm star-shaped polymer. However, the two-arm P3HT chains of high molecular weight (about 9000–10 000 g mol^{-1}) tend to aggregate and appeared as an insoluble form (below 10 wt% of the crude product), which was removed via filtration through Celite and the re-dissolution processes. This was also confirmed by the absence

of the signal corresponding to the benzene protons adjacent to the dioxaborolane groups at 7.70 ppm in the ^{1}H NMR spectrum of s-P3HT-TPA. The further step of washing the product by acetone only removed the unreacted core and oligomers (three-arm stars with short arms), but not the linear P3HT contaminant. It should be mentioned that the peak of the P3HT chain-end proton overlapped with the signal of the internal thienyl ring of non-regioregular P3HT chains. Nevertheless, from the integration ratio of the repeating units of P3HT (peak 1 at 0.94 ppm or peak 7 at 6.96 ppm, Fig. 2(A)) versus the TPA core unit (peak 8 at 7.61 ppm, Fig. 2(A)) and the average M_n of P3HT of 4500 g mol^{-1}, the ratio between the number of P3HT chains and the number of cores was estimated to be 3.2. This suggests that the product contained about 6% of linear P3HT chain contaminant.

In addition, the structure of s-P3HT-TPA was confirmed via the ^{13}C NMR spectrum in Fig. 2(B), which shows all the characteristic peaks of P3HT as well as peaks at 119, 126 and 142 ppm corresponding to the carbons of the TPA core.

Using a similar pathway, s-P3HT-TPB (**9**) was prepared via the Suzuki coupling reaction between P3HT (**3**) and dioxaborolane-containing TPB (**7**) with a yield of 91%. Similarly to the synthesis of s-P3HT-TPA, a P3HT (4500 g mol^{-1}) to dioxaborolane-TPB molar ratio of 1 to 0.3 was employed. The star-shaped structure of s-P3HT-TPB was characterized via ^{1}H NMR and ^{13}C NMR spectra. As shown in Fig. 3(A), all the characteristic peaks of P3HT are clearly observed, while the signals of the TPB core are found at 7.60, 7.47 and 7.42 ppm. From a comparison of the ^{1}H NMR spectra of s-P3HT-TPB and dioxaborolane-TPB, the peak at 7.93 ppm (Fig. 1(B), peak g) related to the protons of the benzene ring adjacent to the dioxaborolane group was shifted to 7.47 ppm for s-P3HT-TPB (Fig. 3(A), peak 8). The crude product obtained was purified similarly to s-P3HT-TPA to eliminate two-arm chains, the unreacted core material and oligomers by filtration through Celite and the re-dissolution and washing processes. The elimination of the two-arm chains and the unreacted dioxaborolane-TPB was confirmed by the absence of the signal corresponding to the benzene protons adjacent to the dioxaborolane groups at 7.93 ppm in the ^{1}H NMR spectrum of s-P3HT-TPB. Taking into account the known M_n of P3HT of 4500 g mol^{-1}, an estimation of the integration ratio between the repeating units of P3HT (peak 1 at 0.94 ppm or peak 7 at 6.96 ppm, Fig. 3(A)) and the TPB protons (peak 10 at 7.60 ppm, Fig. 3(A)) resulted in a P3HT chain-to-core molar ratio of 3.3. This suggests that the product contained about 9% of linear P3HT chain contaminant.

In addition, all ^{13}C NMR characteristic signals of P3HT and the TPB core, indicated by the peaks at 120.5, 127, 129 and 135.5 ppm, confirmed the successful coupling reaction (Fig. 3(B)).

The number-average molecular weights (M_n) as determined by GPC relative to polystyrene standards of s-P3HT-TPA and s-P3HT-TPB were 6000 g mol^{-1} and 7200 g mol^{-1}, with polydispersity indexes ($Đ$) of 1.55 and 1.23, respectively. The single distributions of the molecular weights, shown in Fig. 4, suggest successful Suzuki coupling reactions providing the star-shaped structures. Moreover, these star-shaped P3HTs were very soluble in common organic solvents such as $CHCl_3$, THF, toluene, CH_2Cl_2 and were insoluble in methanol and *n*-heptane. For insight into the structure of the polymers, their intrinsic viscosities [η] were collected from the SEC data as shown in Table 1.

The [η] values of the s-P3HT-TPA and s-P3HT-TPB prepared in the present study were lower than that of linear P3HT with a similar molecular weight, suggesting the existence of a branching

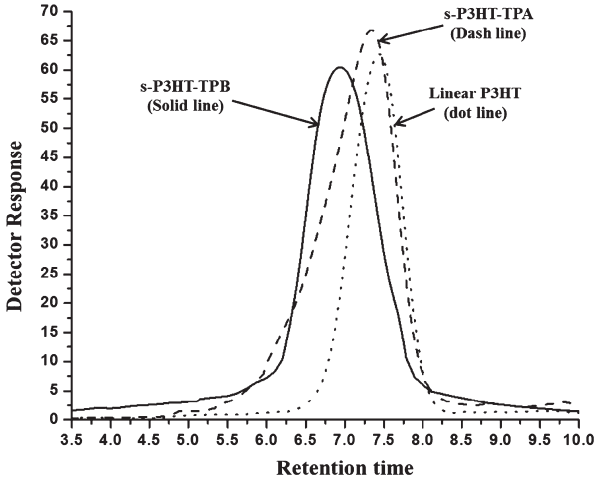

Figure 4. GPC traces of linear P3HT, s-P3HT-TPA and s-P3HT-TPB.

Table 1. Macromolecular characterization of the star-shaped P3HTs with a comparison of the shrinking factor *g*′ as a function of number of arms

Type of polymers	M_n[a] (g mol^{-1})	$Đ = M_w/M_n$	[η] (dg L^{-1})	*g*′	No. of arms
Linear P3HT	4500	1.18	0.127	1	1
s-P3HT-TPA	6000	1.55	0.092	0.72	3.9
s-P3HT-TPB	7200	1.23	0.098	0.77	3.4

[a] The molecular weight (M_n) was determined by SEC.

architecture. The shrinking factor for the intrinsic viscosity of branched polymers, *g*′, can be denoted by

$$g' = \left[\eta\left[_{Br}/\right]\eta\right]_{Lin} \quad (1)$$

here, we denote the intrinsic viscosities of branched and linear polymers with the same molecular weight by $[\eta]_{Br}$ and $[\eta]_{Lin}$. The equation has been extended for coiled polymers in a theta solvent by Roovers.[37] Consistently, $CHCl_3$ is the theta solvent for rigid polymers such as P3HT.

$$g_\eta^\theta\,(\text{empirical}) \approx \left[(3f-2)/f^2\right]^{0.58} \quad (2)$$

Douglas *et al.*[38] have developed an empirical relationship between *g*′ and *f* (where *f* is the number of arms) as

$$g_\eta^*\,(\text{empirical}) \approx g_\eta^\theta\left[1 - 0.267 - 0.015\,(f-1)\right]/(1 - 0.276)$$
$$= \left[(3f-2)/f^2\right]^{0.58}(1 - 0.02f) \quad (3)$$

Using Eqn (3), the *f* values were estimated to be 3.9 and 3.4 for s-P3HT-TPA and s-P3HT-TPB, respectively, which clearly differ from that of linear P3HT. This indicates that star-shaped P3HT polymers were obtained.

Optical properties of s-P3HT-TPA and s-P3HT-TPB

Figures 5(A) and 5(B) depict the UV – visible spectra of s-P3HT-TPA and s-P3HT-TPB, respectively, measured in different solvents and in solid state films. In non-polar (or poorly polar) solvents such as THF, $CHCl_3$ and toluene, the s-P3HT-TPA solutions showed

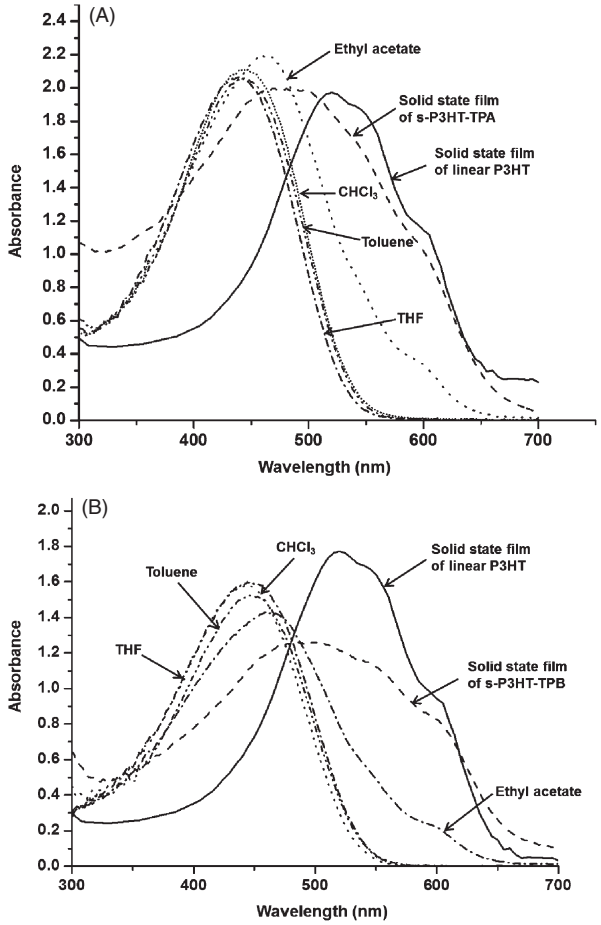

Figure 5. UV – visible spectra of s-P3HT-TPA (A) and s-P3HT-TPB (B) in different solvents and in solid state films.

absorption maxima at around 442 nm attributable to the $\pi - \pi^*$ transition of P3HT moieties. However, in a more polar solvent such as ethyl acetate, the absorption maximum of s-P3HT-TPA was shifted to 464 nm with a small shoulder at 597 nm related to an aggregation of polymer chains. The solid state film of s-P3HT-TPA showed an absorption maximum at 487 nm, which is blue-shifted compared to the absorption maximum at 523 nm of linear P3HT. This observation indicates a low aggregation degree of s-P3HT-TPA in the thin film state as a result of the star-shaped structure. On the other hand, s-P3HT-TPB solutions also showed absorption maximum peaks at around 443 nm corresponding to the $\pi - \pi^*$ transition of P3HT in toluene, $CHCl_3$ and THF, and at 461 nm in ethyl acetate (Fig. 5(B)). The solid state film of s-P3HT-TPB exhibited an absorption maximum at 510 nm, which is more bathochromic than that of s-P3HT-TPA and slightly more hypsochromic than that of linear P3HT. This indicates that in the solid state s-P3HT-TPB is less aggregated than linear P3HT but appears more aggregated than s-P3HT-TPA.

The photoluminescent spectra of s-P3HT-TPA and s-P3HT-TPB in solid state films excited at their absorption maxima, i.e. 487 and 510 nm respectively, are shown in Fig. 6. In solid state films, both s-P3HT-TPA and s-P3HT-TPB as well as linear P3HT displayed an emission peak at 727 nm. However, the star-shaped P3HTs exhibited an additional peak at around 380 nm, attributed to the TPA/TPB core. It is suggested that the quantum yields of the star-shaped P3HTs were similar to that of linear P3HT.

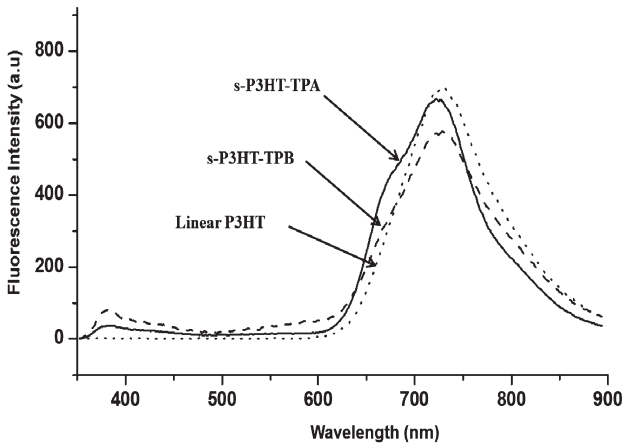

Figure 6. Fluorescence spectra of s-P3HT-TPA and s-P3HT-TPB in solid films excited at 487 nm and 510 nm, respectively.

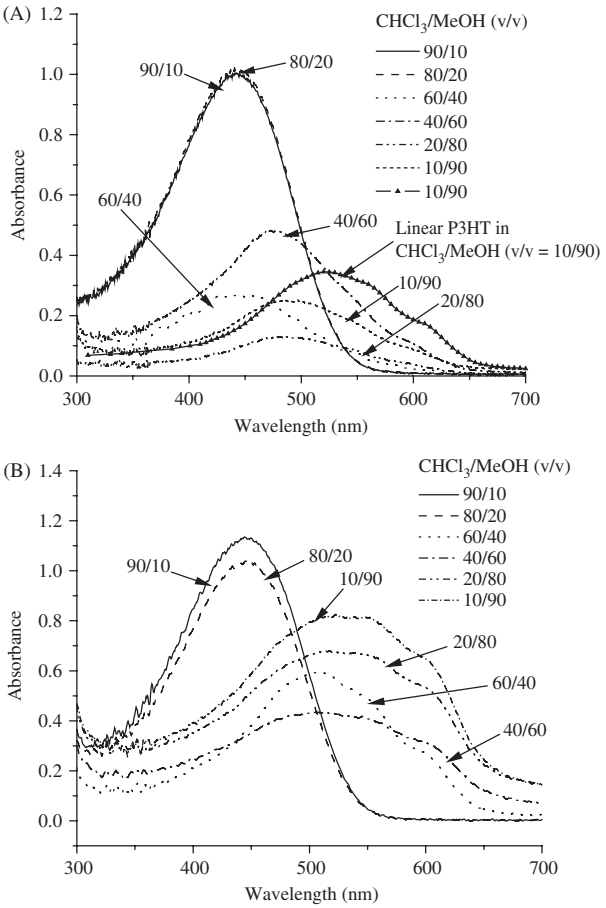

Figure 7. UV – visible spectra of s-P3HT-TPA (A) and s-P3HT-TPB (B) measured in $CHCl_3$/MeOH mixtures with various compositions.

Solvent-induced aggregation of s-P3HT-TPA and s-P3HT-TPB

The intermolecular interactions based on π-stacking in the solid state have a significant effect on the aggregation of conjugated polymers, which induces changes in their optical properties. The exciton model can be used to explain the optical properties induced by intermolecular interactions.[39] The aggregates in solution, including H-aggregates (with parallel aligned transition dipoles) and J-aggregates (with head-to-tail aligned

transition dipoles), exhibit distinct changes in the absorption band, i.e. bathochromic (red) shifts or hypsochromic (blue) shifts, respectively, compared to the monomeric species.[40] Molecular aggregation can possibly be induced by the addition of a non-solvent to a polymer solution. Figure 7 displays the absorption spectra of s-P3HT-TPA and s-P3HT-TPB, measured in $CHCl_3$/methanol mixtures. The $\pi - \pi^*$ absorption band of s-P3HT-TPA is located at 448 nm in pure $CHCl_3$, indicating a coil conformation of polymer chains. The addition of methanol from 10% to 90% to polymer solutions led to red shifts of the absorption maximum, which was located at 500 nm for the 10/90 $CHCl_3$/methanol solution. It should be noted that in the same solvent mixture linear P3HT exhibited a $\pi - \pi^*$ absorption maximum at 530 nm (Fig. 7(A)). The more hypsochromic feature in the absorption spectrum of s-P3HT-TPA, compared to that of linear P3HT, indicated that the star structure of s-P3HT-TPA induced a decrease of polymer chain aggregation.

Contrastingly, s-P3HT-TPB exhibited a $\pi - \pi^*$ absorption band at 530 nm in a $CHCl_3$/methanol mixture with 90% content of methanol, which is similar to that of linear P3HT. This suggests that the core structure has a strong impact on the molecular aggregation, although the number of arms and arm length were the same. Benefiting from the special propeller-like starburst molecular structure of the TPA core as a result of the sp3 hybrid orbital of the nitrogen atom, s-P3HT-TPA shows weak intermolecular interactions and hence substantially reduced molecular aggregation. In contrast, despite the starburst molecular architecture of s-P3HT-TPB, the planar structure of the TPB core favors more intermolecular interactions than s-P3HT-TPA.

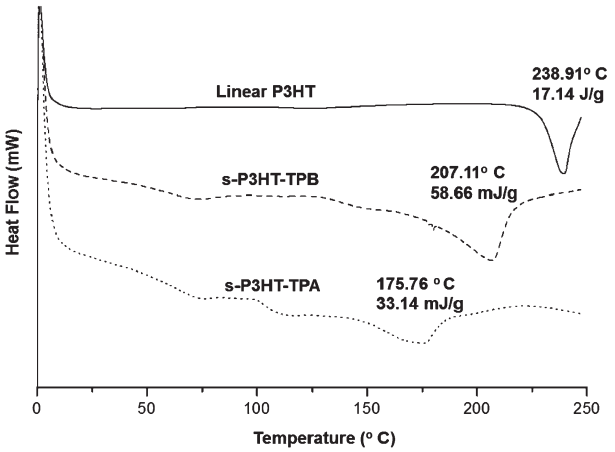

Figure 8. DSC second-heating traces (exo up) of linear P3HT, s-P3HT-TPA and s-P3HT-TPB.

Thermal properties of s-P3HT-TPA and s-P3HT-TPB

The thermal properties of the star-shaped P3HTs were studied via DSC. The DSC second-heating traces in the range from 0 to 250 °C of the star-shaped P3HTs are shown in Fig. 8. Melting peaks at 238.9, 207.1 and 175.76 °C were observed for linear P3HT, s-P3HT-TPB and s-P3HT-TPA, respectively. It is well known that linear P3HT chains are generally stiff chain molecules with very strong intermolecular interactions, resulting in high melting temperatures normally above 200 °C. It is obvious that the star-shaped structure hinders the stacking of P3HT chains, giving rise to decreased chain aggregation. In the order from P3HT,

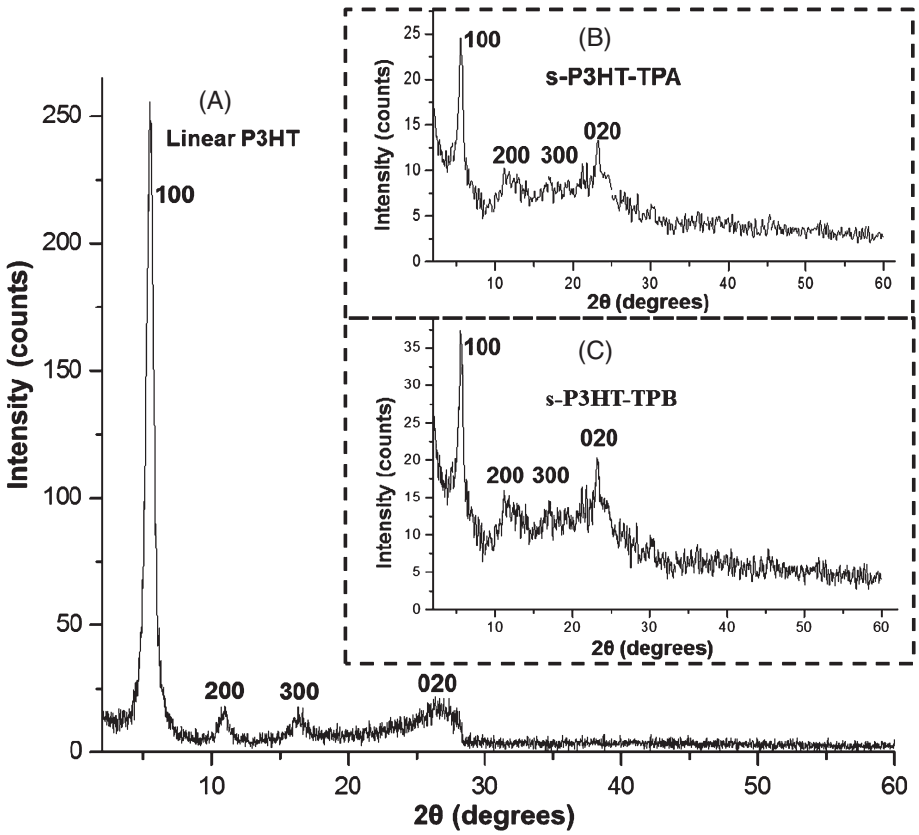

Figure 9. XRD patterns of linear P3HT, s-P3HT-TPA and s-P3HT-TPB.

s-P3HT-TPB to s-P3HT-TPA, the decreases in melting temperature as well as in melting enthalpy indicate decreases in the crystallization of P3HT chains. In addition, s-P3HT-TPA showed a glass transition at 105 °C originating from the disordered phase of P3HT arm chains. This suggests a considerably lower order of chain stacking of s-P3HT-TPA in comparison with s-P3HT-TPB, which is in good agreement with the above UV – visible results.

Solid structure of s-P3HT-TPA and s-P3HT-TPB

The optoelectronic property of thiophene-based conjugated polymers is strongly related to their structural order in the solid state.[41,42] Thus, it is of critical importance to assess the morphology of conjugated polymers for successful application of these materials in organic optoelectronics. The molecular order of the star-shaped P3HTs in the solid state was investigated by powder XRD measurements (Fig. 9). The XRD pattern of linear P3HT revealed the characteristic reflection peaks observed for classical P3HT materials.[43–45] These include the $d(100)$ reflection peak at $2\theta = 5.6°$ attributed to an interlayer spacing of 15.8 Å between linear conjugated segments separated by *n*-hexyl side chains, and the $d(020)$ peak at $2\theta = 26.4°$ corresponding to the $\pi - \pi$ stacking spacing of 3.4 Å between P3HT chains within the main chain layers. The XRD patterns of the star-shaped P3HTs also showed characteristic (100) and (020) reflections typical of P3HT chains at 5.6° and 23.9°, respectively. The larger $d(020)$ value, of 3.7 Å ($2\theta = 23.9°$), compared to that of the linear P3HT revealed a larger $\pi - \pi$ stacking distance between the P3HT arm chains due to lower intermolecular interactions. In addition, the intensities of these peaks were about 10 times lower than those of linear P3HT, indicating much lower degrees of polymer chain aggregation in the structure of the star-shaped polymers. From a comparison of the XRD patterns of s-P3HT-TPA and s-P3HT-TPB, the somewhat lower intensities of the main reflections of s-P3HT-TPA agreed well with the fact that s-P3HT-TPA has a lower order of chain stacking than s-P3HT-TPB.

CONCLUSIONS

In this research, we have demonstrated the synthesis of star-shaped P3HTs containing TPA or TPB as the core via the Suzuki coupling reaction. The molecular weights of the star-shaped polymers obtained were in the range 6000 – 7200 g mol^{-1} with a shrinking factor g' lower than that of the corresponding linear P3HT. It was found that the core structure plays a critical role in the aggregation of P3HT chains and hence optical properties, as evidenced by the UV – visible, DSC and XRD results. A propeller-like core structure, such as that of TPA, resulted in a star-shaped P3HT with much lower order of chain stacking than one with a planar geometry core.

ACKNOWLEDGEMENTS

This research was fully supported by Vietnam National Foundation for Science and Technology Development (NAFOSTED) under grant number 104.02-2013.18.

REFERENCES

1 Simpson CD, Wu J, Watson MD and Mullen K, *J Mater Chem* **14**:494 – 504 (2004).
2 Grimsdale AC and Müllen K, *Chem Rec* **1**:243 – 257 (2001).
3 Zhang WB, Jin WH, Zhou XH and Pei J, *Tetrahedron* **63**:2907 – 2914 (2007).
4 Okumoto K and Shirota Y, *Chem Mater* **15**:699 – 707 (2003).
5 Lu J, Tao Y, D'Iorio M, Li Y, Ding J and Day M, *Macromolecules* **37**:2442 – 2449 (2004).
6 Kanibolotsky AL, Perepichka IF and Skabara PJ, *Chem Soc Rev* **39**:2695 – 2728 (2010).
7 Roncali J, Leriche P and Cravino A, *Adv Mater* **19**:2045 – 2060 (2007).
8 Novoselov KS, Geim AK, Morozov SV, Jiang D, Zhang Y, Dubonos SV *et al., Science* **306**:666 – 669 (2004).
9 Novoselov KS, Geim AK, Morozov SV, Jiang D, Katsnelson MI, Grigorieva IV *et al., Nature* **438**:197 – 200 (2005).
10 Geim AK and Novoselov KS, *Nat Mater* **6**:183 – 191 (2007).
11 Geim AK, *Science* **324**:1530 – 1534 (2009).
12 Liu TA, Prabhakar C, Yu JY, Chen Ch, Huang HH and Yang JS, *Macromolecules* **45**:4529 – 4539 (2012).
13 Wang F, Wilson MS, Rauh RD, Schottland P, Thompson BC and Reynolds JR, *Macromolecules* **33**:2083 – 2091 (2000).
14 Schulz GL, Mastalerz M, Ma CQ, Wienk M, Janssen R and Bäuerle P, *Macromolecules* **46**:2141 – 2151 (2013).
15 Hsu JC, Sugiyama K, Chiu YC, Hirao A and Chen WC, *Macromolecules* **43**:7151 – 7158 (2010).
16 Tomović Ž, Dongen Jv, George SJ, Xu H, Pisula W, Leclère P *et al., J Am Chem Soc* **129**:16190 – 16196 (2007).
17 Chakraborty C, Layek A, Ray PP and Malik S, *Eur Polym J* **52**:181 – 192 (2014).
18 Kanibolotsky AL, Berridge R, Skabara PJ, Perepichka IF, Bradley DDC and Koeberg M, *J Am Chem Soc* **126**:13695 – 13702 (2004).
19 Li W, Li Q, Duan C, Liu S, Ying L, Huang F *et al., Dyes Pigm* **113**:1 – 7 (2015).
20 Cheng X, Zhao J, Cui C, Fu Y and Zhang X, *J Electroanal Chem* **677 – 680**:24 – 30 (2012).
21 Ren S, Zeng D, Zhong H, Wang Y, Qian S and Fang Q, *J Phys Chem B* **114**:10374 – 10383 (2010).
22 Zhou XH, Yan JC and Pei J, *Org Lett* **5**:3543 – 3546 (2003).
23 Hoang MH, Cho MJ, Kim DC, Kim KH, Shin JW, Cho MY *et al., Org Electron* **10**:607 – 617 (2009).
24 Takamizu K and Nomura K, *J Am Chem Soc* **134**:7892 – 7895 (2012).
25 Tkachov R, Senkovskyy V, Horecha M, Oertel U, Stamm M and Kiriy A, *Chem Commun* **46**:1425 – 1427 (2010).
26 Tkachov R, Senkovskyy V, Oertel U, Synytska A, Horecha M and Kiriy A, *Macromol Rapid Commun* **31**:2146 – 2150 (2010).
27 Jana D and Ghorai BK, *Tetrahedron Lett* **53**:1798 – 1801 (2012).
28 Roquet S, Cravino A, Leriche P, Alévêque O, Frère P and Roncali J, *J Am Chem Soc* **128**:3459 – 3466 (2006).
29 Niamnont N, Kimpitak N, Wongravee K, Rashatasakhon P, Baldridge KK, Siegel JS *et al., Chem Commun* **49**:780 – 782 (2013).
30 Zhang J, Deng D, He C, He Y, Zhang M, Zhang ZG *et al., Chem Mater* **23**:817 – 822 (2010).
31 Paek S, Cho N, Cho S, Lee JK and Ko J, *Org Lett* **14**:6326 – 6329 (2012).
32 Hu Z, Li Wd, Zhang W, Liang A, Ye D, Liu Z *et al., RSC Adv* **4**:5591 – 5597 (2014).
33 Yu G, Gao J, Hummelen JC, Wudl F and Heeger AJ, *Science* **270**:1789 – 1791 (1995).
34 Thompson BC and Fréchet JMJ, *Angew Chem Int Ed* **47**:58 – 77 (2008).
35 Yuan M, Okamoto K, Bronstein HA and Luscombe CK, ACS *Macro Lett* **1**:392 – 395 (2012).
36 Senkovskyy V, Beryozkina T, Bocharova V, Tkachov R, Komber H, Lederer A *et al., Macromol Symp* **17 – 25**:291 – 292 (2010).
37 Roovers J, Branched polymers, in *Encyclopedia of Polymer Science and Engineering*, ed. by Kroschwitz JI. Wiley-Interscience, New York, vol. 2, pp. 478 – 499 (1985).
38 Douglas JF, Roovers J and Freed KF, *Macromolecules* **23**:4168 – 4180 (1990).
39 DiCésare N, Belletête M, Garcia ER, Leclerc M and Durocher G, *J Phys Chem A* **103**:3864 – 3875 (1999).
40 Ruini A, Caldas M, Bussi G and Molinari E, *Phys Rev Lett* **88**:206 – 403 (2002).
41 Fichou D, *J Mater Chem* **10**:571 – 588 (2000).
42 Hu Z, Liu J, Simón-Bower L, Zhai L and Gesquiere AJ, *J Phys Chem B* **117**:4461 – 4467 (2013).
43 Zen A, Saphiannikova M, Neher D, Grenzer J, Grigorian S, Pietsch U *et al., Macromolecules* **39**:2162 – 2171 (2006).
44 Chen TA, Wu X and Rieke RD, *J Am Chem Soc* **117**:233 – 244 (1995).
45 Nguyen HT, Nguyen LT, Nguyen T, Luu TA and Van Le T, *J Polym Res* **21**:1 – 11 (2014).

